Creating an Optical Feedback Loop to Probe Dynamics of Quantum Fluids of Light in Disorder Potential

Submitted by:

Sagnik Ghosh

Indian Institute of Science Education and Research, Pune

Supervised by:

Dr. Quentin Glorieux

Laboratoire Kastler Brossel,

Sorbonne Universite, ENS, College de France, Paris

Contents

List of Figures

Chapter 1

The Interferometer

1.1 Introduction

The stated purpose of the project was to set up an optical feedback loop, given a black-box, that would reproduce the information of phase and intensity distribution of the output plane to its input plane. The usefulness of such a set up is enormous. The current motivation draws in from a proposed study of dynamics of Quantum superfluids of light in a disorder potential. The LKB group is an expert in quantum optics and quantum fluids [**?**, **?**, **?**, **?**]. Recently the lab has shown the Bogoliubov dispersion in quantum fluids of super fluids of light. This system is achieved by sending a laser beam through a non-linear medium, in our case Rb vapors. The non-linear optics is governed by 3-D non-linear Maxwell equations, which can be mapped to a 2D Gross-Pitaevskii equation by identifying z axis of the previous with time axis of the second. Thus in our cell, every slice in x-y plan, that is the planes perpendicular to the incident beams different segments of time for the *fluid dynamics*. However in an optical setup the data is snapshot by a camera and it is not possible to setup one inside the Rb vapor cell. As well as, any applied potential, that is time independent should be constant in z-axis, and thus diffraction-less, which is hard to set up. Presence of a feedback loop solves both this problem. We record data at one plan and when we feed it back as input, accurately, we are virtually reproducing the next part of the experiment. (that is the next segment of same length of the blackbox, or in other words, after same interval; for the fluid dynamical quantities.) Running the loop n-times basically gives us a cell of length n-times of the black box length, with data recorded after every unit length. Thus for example, in the aforementioned experiment of dynamics of disorder potential, the length for which the potential is supposed to remain diffraction-less also decreases by n-folds.

1.2 Interferometer set up

The interferometer essentially consists of two arms, one reference and one test. The first beam spliter breaks the beam into two beams of equal intensity. The refracted part is fed into the main interferometer. The main interferometer is constructed of two beam splitters and two mirrors and creates two parallel running arms of equal length. The right one is used as reference arm, and we place the black-box in the left one to create the test arm. All splitters used here are 50-50 non-polarizing splitter. Since,

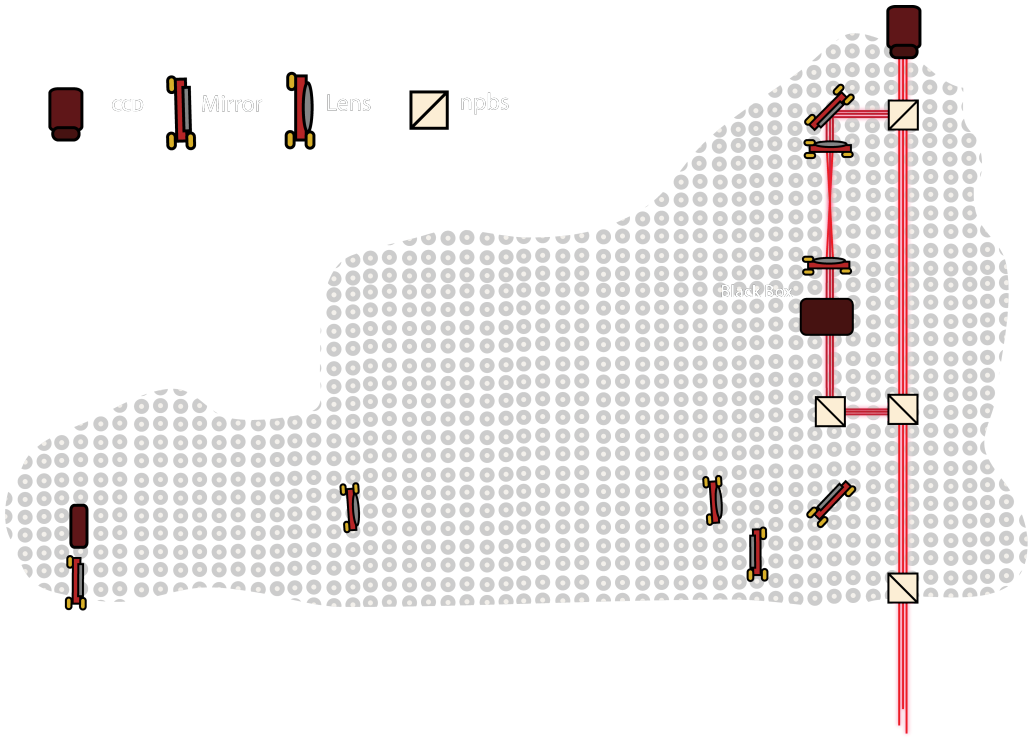

(a) The main interferometer

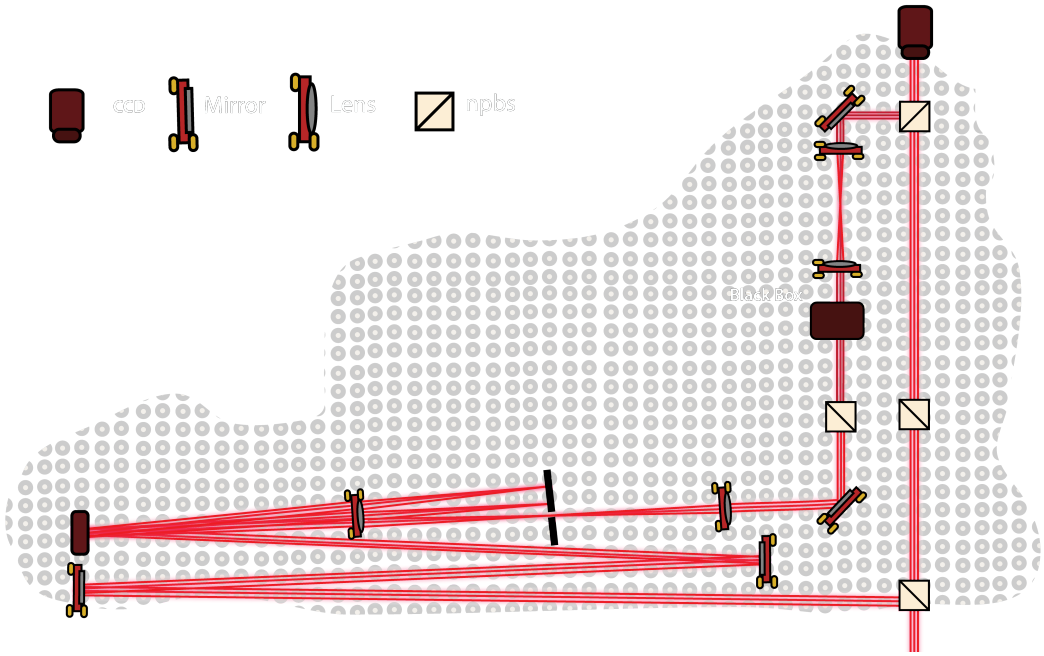

(b) The Ray diagram

Figure 1.1: The complete setup.

both the reference beam and the test beam runs through same number of splitters, they are supposed to have similar intensity in the camera, barring the intensity loss in the mirrors. The output plane is conjugated to the camera plane by using two 15 cm lens in 4f set up. This creates an inverted image of the output plane with magnification 1. The idea is to then feedback this info using an Spatial Light Modulator (SLM).

spatial light modulator is an array of micro-mirrors each of which can be individually rotated in an angle between $[0, 2\pi]$ The SLM requires a grayscale image of same dimensions as of the array where each pixel can take values between [0,255] the SLM than maps this values to the mirror phase after appropriate re-scaling. We impart a grating along with the phase map obtained from the previous loop to filter the first order. A telescope is setup using two 10cm lens in 4f setup to map the SLM plane to the input. There is a gap of 5 cm between the input and output planes of the black-box. For the purpose of the experiment we use a converging 50 cm lens, to mimic the black-box. The grating height is modulated to control the beam size by exploiting selective diffraction.

Chapter 2

Phase Extraction

Over here we discuss in detail the algorithm and the its nitty-gritties, for the extraction of the phase information from an interference pattern of two coherent beams. The purpose of the phase extraction is to feedback this information from the output of one run of the loop as the input of the next run using an Spatial Light Modulator (SLM). For this reason, attempts has been made to make the code as general, robust and accurate as possible. The current version of the algorithm does not involve any parameter, does not assume any symmetry of the interferogram, and does not require any post-processing. As output, it provides us with the information of phase and curvature at each pixel as arrays.

2.1 Theory

The underlying theory for the phase extraction code is that of interference of two coherent beams. Each of the beams, as is captured by the camera, can be thought of as an array with each pixel having information of phase and intensity. The aim of the code is to extract the phase info of the test beam, by interfering it with the standard one.

Let, the field vectors be

$$\text{for the reference beam:} E_1(m,n)e^{i\Phi_1(m,n)}$$
$$\text{for the test beam:} E_2(m,n)e^{i\Phi_2(m,n)}$$

$$\text{therefore, for the interference pattern:} E_1(m,n)e^{i\Phi_1(m,n)} + E_2(m,n)e^{i\Phi_2(m,n)}$$

The camera however only records the modulus square, that is,

$$\text{for the reference beam:} I_1(m,n) = E_1(m,n)^2$$
$$\text{for the test beam:} I_2(m,n) = E_2(m,n)^2$$

therefore, for the interference pattern:

$$I = I_1(m,n) + I_2(m,n) + 2\sqrt{I_1(m,n) * I_2(m,n)}cos(\Delta\Phi(m,n)); \tag{2.1}$$
$$\Delta\Phi(m,n) = \Phi_1(m,n) - \Phi_2(m,n) \tag{2.2}$$

This formula forms the fulcrum of the algorithm. We notice that for each pixel the information of an interference pattern has three independent degrees of freedom, the intensity of both the beams $I_1(m,n), I_2(m,n)$ and the phase difference $\Delta\Phi(m,n)$. Guided by that, any parameter independent phase-extraction algorithm would require three independent readings, Image of the interference pattern (I(m,n)), The reference beam ($I_1(m,n)$) and the test beam ($I_2(m,n)$). Having this three info, we negate from I, the $I_1(m,n)$ and $I_2(m,n)$, which leaves us with the third term. Dividing the third term by $2\sqrt{I_1(m,n) * I_2(m,n)}$, we obtain the phase information. For two plane waves (zero curvature) interfering with each other this term is expected to oscillate between [-1,1]. the phase information is then retrieved by a Arccos which maps it into the range $[0,\pi]$.

The aim of the phase extraction code is to prepare the input data for the SLM. As is discussed in the previous chapter, it is an array of micromirrors which can be rotated in any angle between 0 and Π. So our phase-map, prepared from the phase extraction algorithm also should be unwrapped from half interval $[0,\pi]$ to the full interval $[0,2\pi)$. Cosine function has the following property,

$$\cos(x) = \cos(\pi - x) \tag{2.3}$$

This means that for a phase diagram, the Arccos output is monotonically increasing from 0 to π, which corresponds to variation of the cosine term from 1 to -1 monotonically. Then the cosine term increases from -1 to 1 again, which corresponds to a increase in phase from π to 2π, but in the output of the above algorithm it is represented by a decrease in phase from π to 0, owing to property [2.3] and needs a unwrapping.

We exploit the decreasing nature of the Arccos output to detect the parts of the phase diagram that needs unwrapping and then negate its present value from 2π to have it unwrapped. We first go row-wise (horizontally),

This left to itself, in general, would create discontinuities in the phase in vertical direction. To nullify that a vertical scan is required too. Two sets of scans, however does not over determine the data, as in the unwrapping is ran on only the portions which has a decreasing phase change, and yields a smoothly varying Phase diagram, where phase values ranges from $[0,2\pi)$. In the reported diagrams however we have identified phase angle x and $\pi - x$. For feeding in the SLM we rescale the colormap in greyscale from $[0,2\pi)$ to [0,257] with 257 being the darkest(black) and 0 being the lightest (white).

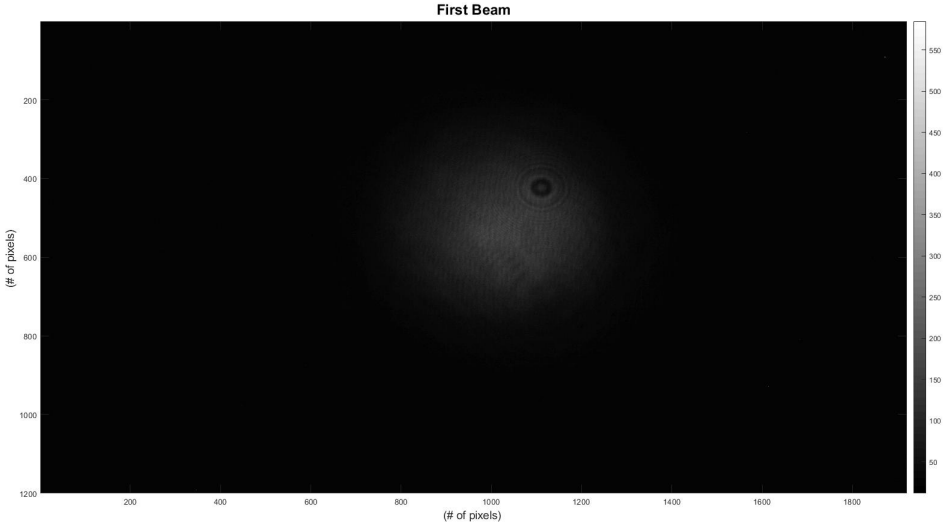

(a) Input reference beam (Beam 1)

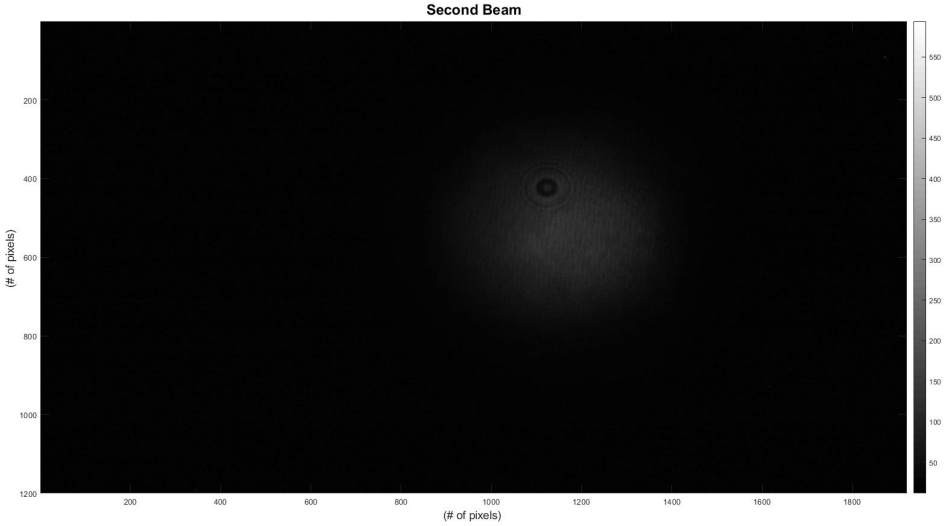

(b) Input test beam (Beam 2)

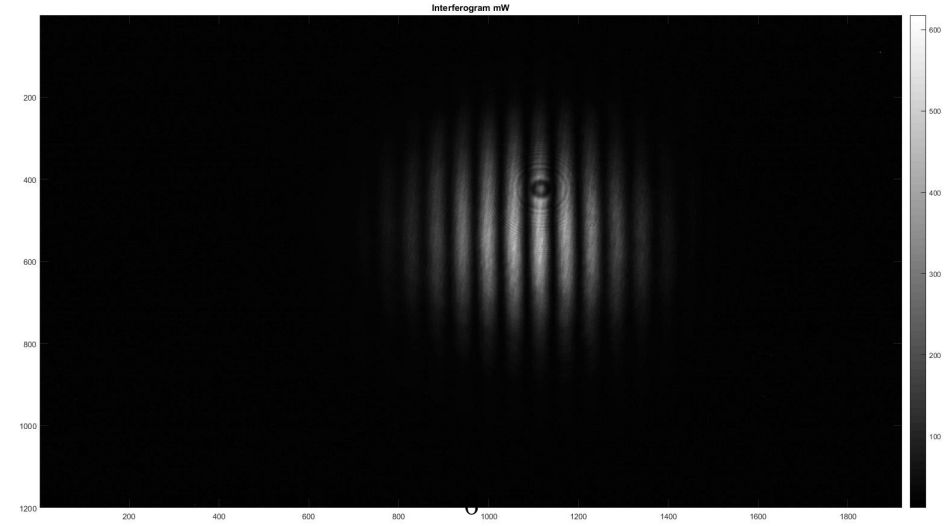

(c) Input inteferogram

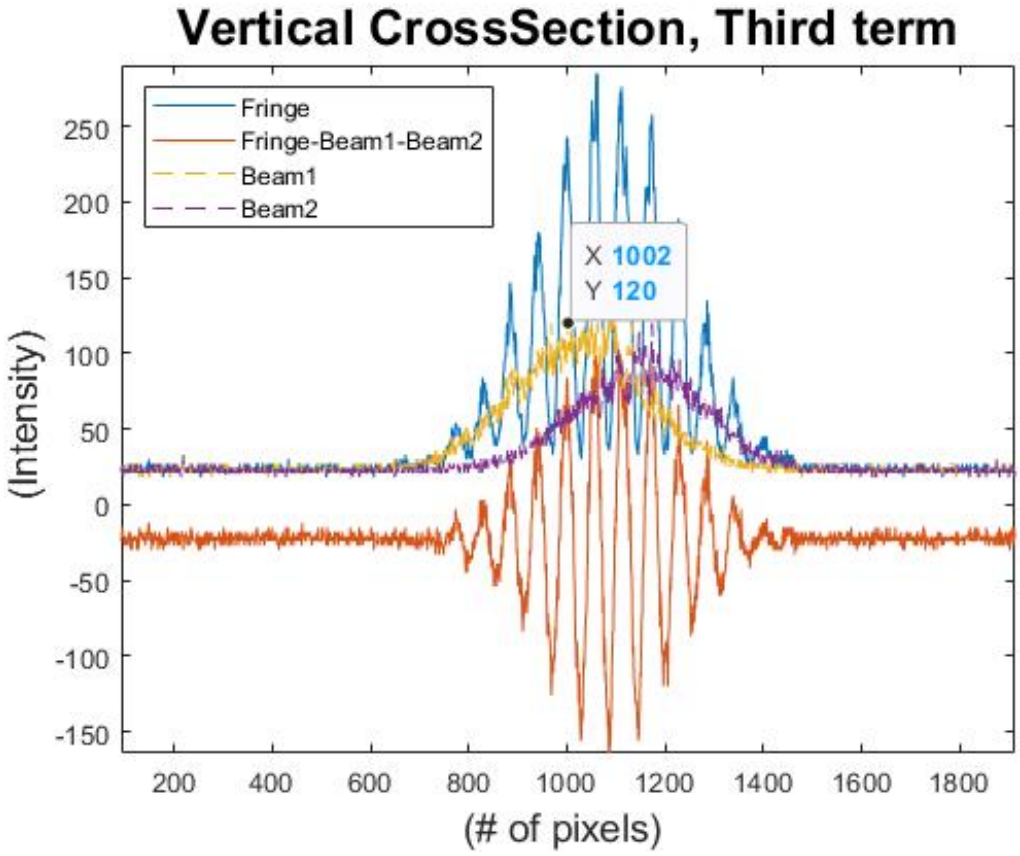

(a) Vertical cross-sections of beam 1, beam 2, interferogram and the third term

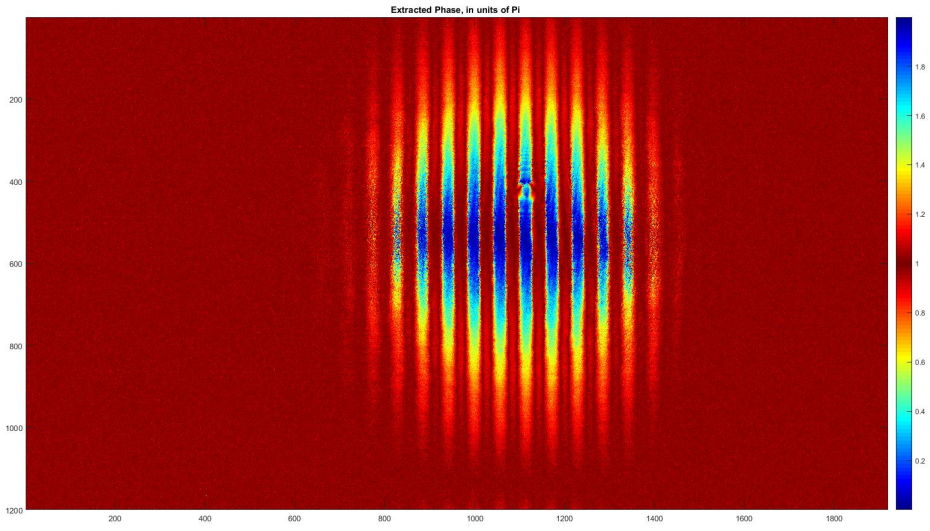

(b) Output phase diagram

Figure 2.2: The functioning of the code: The code takes as input the first three images. We first produce the interference term (third term) by negating beam 1, beam 2 from the interferogram. It is seen to oscillate around a constant background, fig (2.2a). This term is then divided by its envelope to obtain Phase diagram, fig (2.2b). Notice the artifact due to the dirt in fringe, fig (2.1c) is no more present in the phase diagram.

2.2 Results: Handling dirty optics

Here we present the output phase diagrams for fringes of various geometry. Our algorithm The functioning of the code: The code takes as input the first three images. We first produce the interference term (third term) by negating beam 1, beam 2 from the interferogram. It is seen to oscillate around a constant background, fig (2.2a). This term is then divided by its envelope to obtain Phase diagram, fig (2.2b). Notice the artifact due to the dirt in fringe, fig (2.1c) is no more present in the phase diagram.The functioning of the code: The code takes as input the first three images. We first produce the interference term (third term) by negating beam 1, beam 2 from the interferogram. It is seen to oscillate around a constant background, fig (2.2a). This term is then divided by its envelope to obtain Phase diagram, fig (2.2b). Notice the artifact due to the dirt in fringe, fig (2.1c) is no more present in the phase diagram.The functioning of the code: The code takes as input the first three images. We first produce the interference term (third term) by negating beam 1, beam 2 from the interferogram. It is seen to oscillate around a constant background, fig (2.2a). This term is then divided by its envelope to obtain Phase diagram, fig (2.2b). Notice the artifact due to the dirt in fringe, fig (2.1c) is no more present in the phase diagram.The functioning of the code: The code takes as input the first three images. We first produce the interference term (third term) by negating beam 1, beam 2 from the interferogram. It is seen to oscillate around a constant background, fig (2.2a). This term is then divided by its envelope to obtain Phase diagram, fig (2.2b). Notice the artifact due to the dirt in fringe, fig (2.1c) is no more present in the phase diagram.

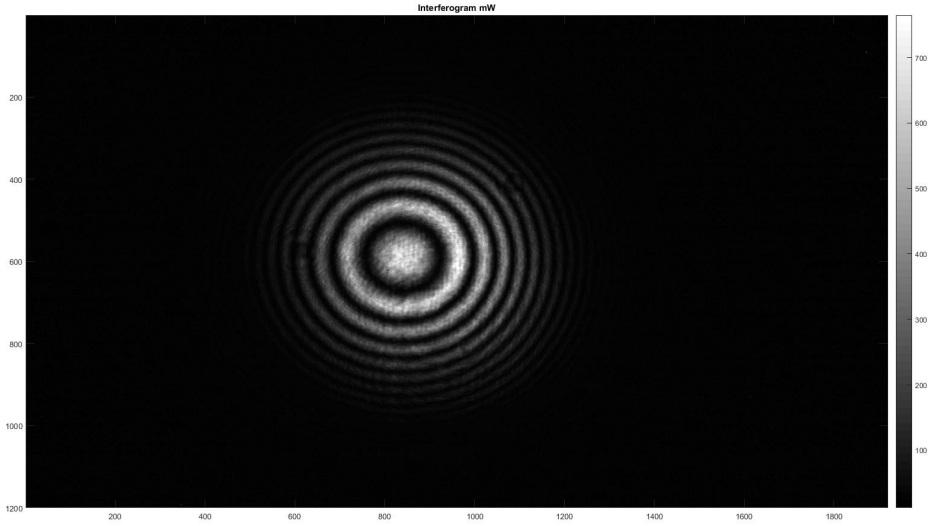

(a) Inteferogram

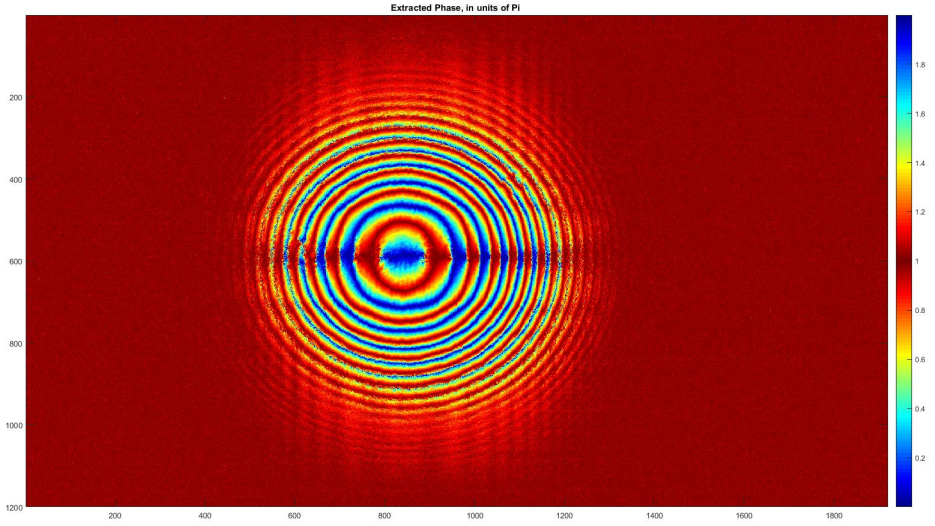

(b) Phase diagram

Figure 2.3: The input interferogram of a sample circular fringe pattern and the extracted phase by the code

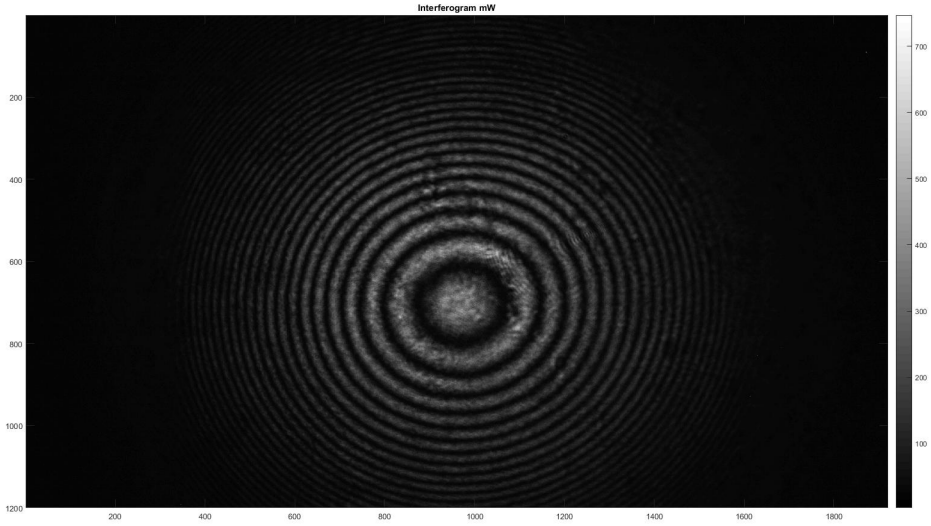

(a) Inteferogram

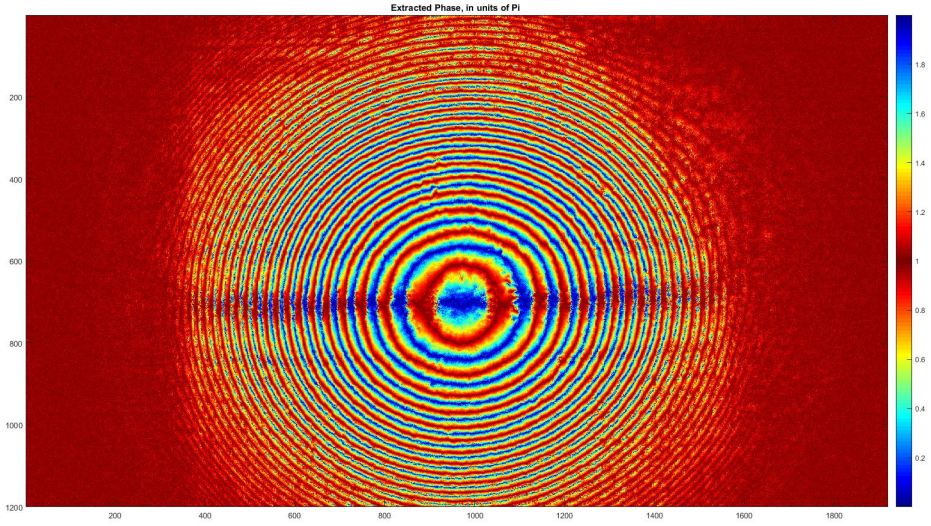

(b) Phase diagram

Figure 2.4: The input interferogram of a sample circular fringe pattern and the extracted phase by the code

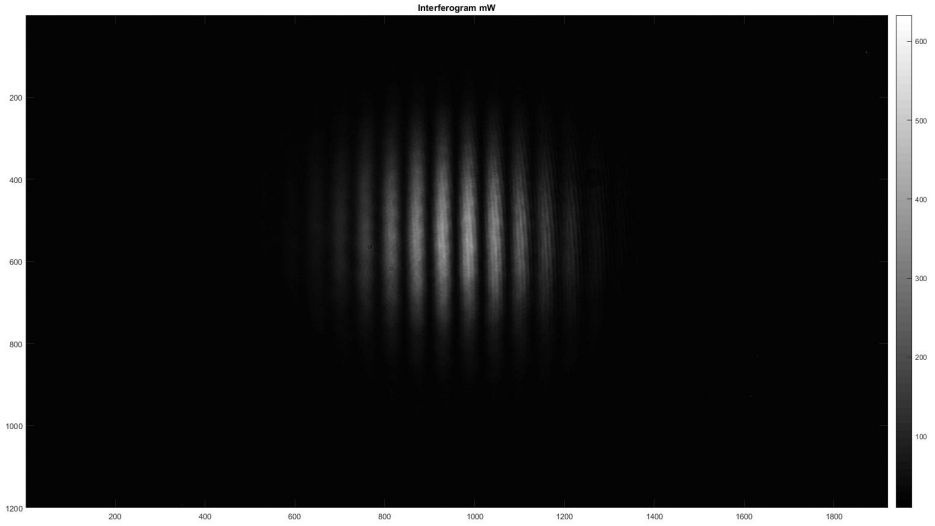

(a) Inteferogram

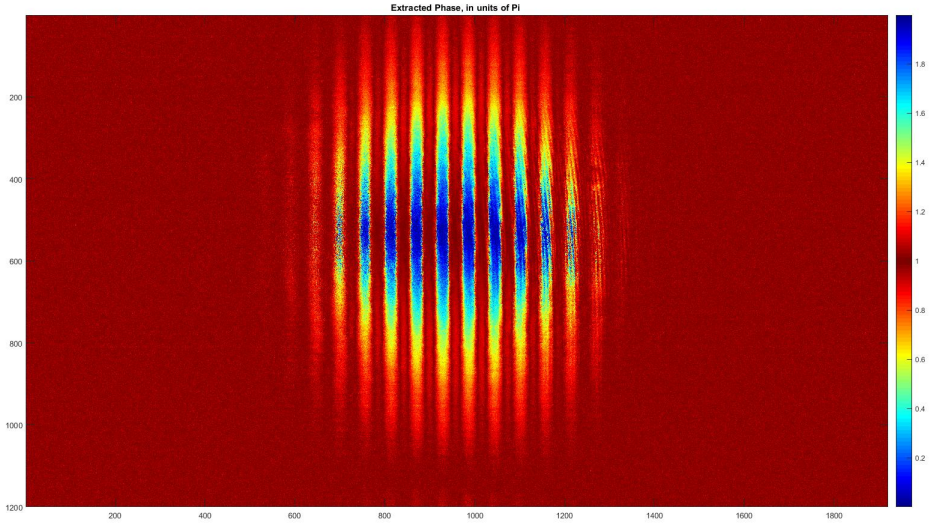

(b) Phase diagram

Figure 2.5: The input interferogram of a sample linear fringe pattern and the extracted phase by the code

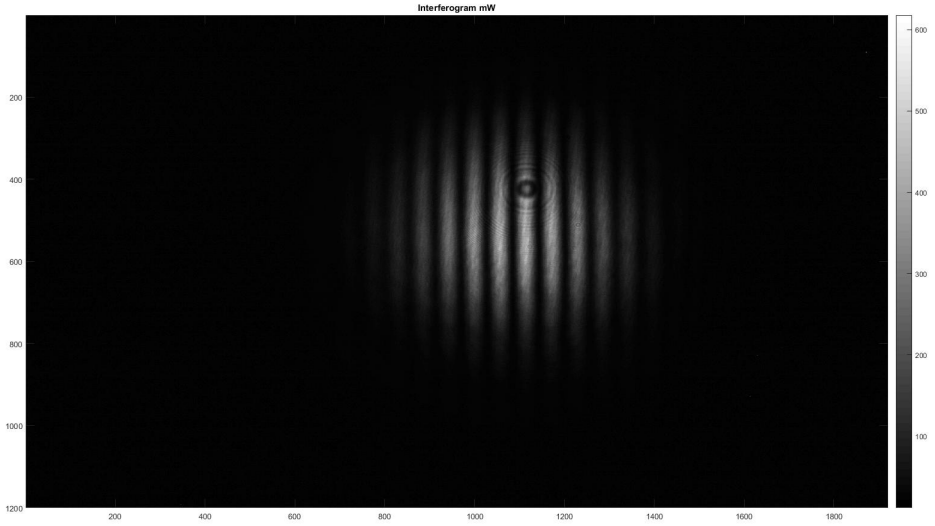

(a) Inteferogram

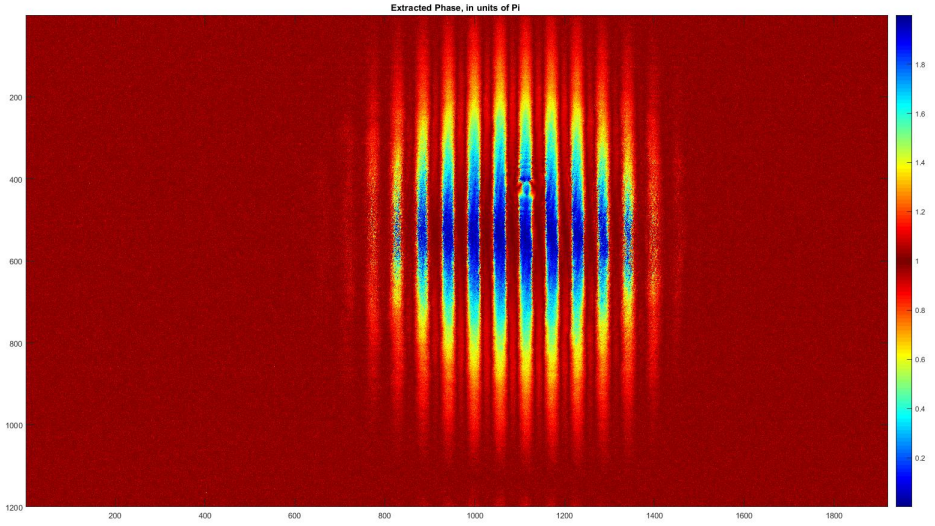

(b) Phase diagram

Figure 2.6: The input interferogram of a sample linear fringe pattern and the extracted phase by the code

Chapter 3

Feedback

Over here we discuss in detail the algorithm and the its nitty-gritties, for the extraction of the phase information from an interference pattern of two coherent beams. The purpose of the phase extraction is to feedback this information from the output of one run of the loop as the input of the next run using an Spatial Light Modulator (SLM). For this reason, attempts has been made to make the code as general, robust and accurate as possible. The current version of the algorithm does not involve any parameter, does not assume any geometry of the interferogram, and does not require any post-processing. As output, it provides us with the information of phase and curvature at each pixel as arrays.

3.1 Results: Trial Runs

In this final section we present the results from the only two trial runs performed. The first run was conducted on June 27, 2019. This set-up carried the following faults. Firstly, one mirror in the path of the test beam was of visible range. This mirror behaves practically as a transmitter in the infrared regime, so intensity was significantly lost, in the test beam. Consequently the ratio of intensity of the test beam vs reference beam is too low, and the results exhibit small signal-to-noise ratio.

During this run, no gratings were used in the SLM. Now, the SLM is not a continuous array of mirrors, and in the zeroth order reflects partly both modulated and unmodulated beams. Imaging the zeroth order directly thus, give rise to two interference patterns instead of one, simultaneously, one due to the phase modulated part, another due to the unmodulated part of the test beam, and are thus inseparable. Both of these patterns however are radially symmetric, and the readings were taken by aligning their centres.

The presence of the unmodulated beam creates error in the phase diagrams, which gets piled up after every run. The run was stopped after fifth loop, as the interference pattern turned out to be too complicated to yield any meaningful, conclusive results.

The spread of the beam is supposed to decrease as we run more and more loops, if we are faithfully reproducing the convergence of a beam. This effect in an ideal case is to be brought in by the DMD, which were not use in the current runs. Therefore, all the beams of the trial run exhibits, similar width. However there is a qualitative trend of increasing intensity resulting from the increase of curvature of the beam at each loop.

Most of these errors were accounted for in the second run. The faulty mirror was replaced and a grating was added in the SLM to maximize the first order output, and it was filtered through a pinhole in the first Fourier plane, as is shown in the interferometer. We also adopted a method to account for the reducing beam size numerically by modulating the grating height and selecting for the first order. The primary problem faced in this case was to numerically modulate the grating, aligning it properly with the center of the input beam to the SLM, and also the geometry of the set up. In the current set up, the seprataion of the optical instruments are far from perfect.

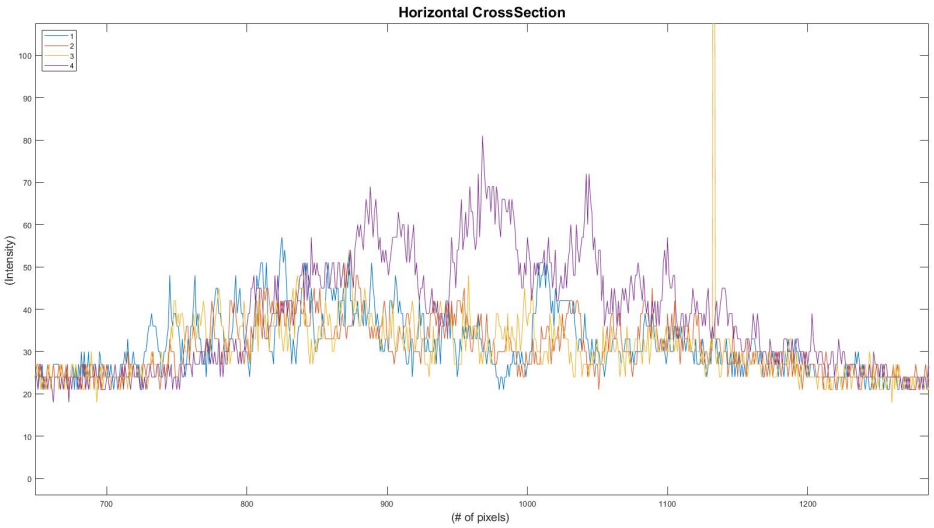

(a) Horizontal cross-section of output beams at various steps

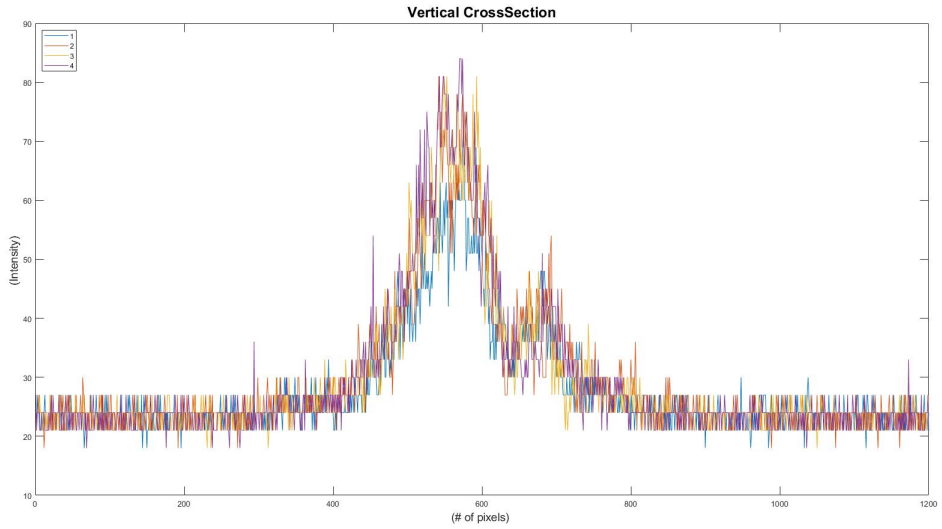

(b) Vertical cross-section of output beams at various steps

Figure 3.1: Trial run 1: This set up had the problem of not accounting for the reducing beam size and loosing intensity due to use of an visible range mirror. Consequently the width of the distribution does not change, and the signal-noise ratio is too low. However, a trend of increasing intensity can be observed resulting from the increasing curvature.

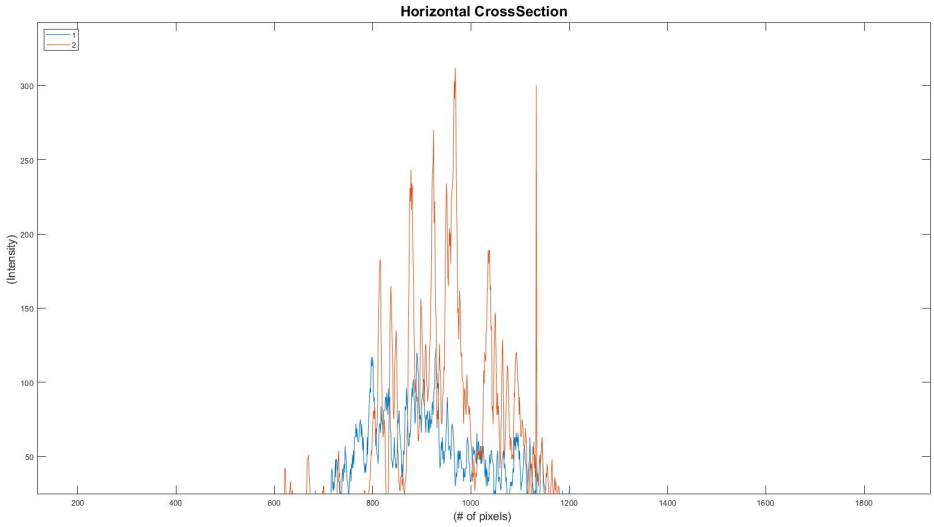

(a) Horizontal cross-section of output beams at various steps

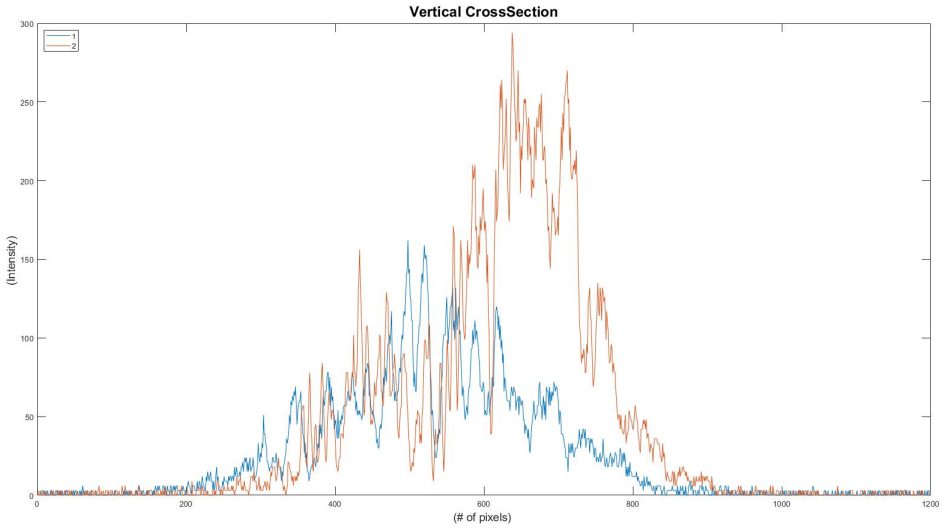

(b) Vertical cross-section of output beams at various steps

Figure 3.2: Trial run 2: Error due to the mirror corrected (shows good signal-to-noise ratio). The correction in beam size is partly accomplished, exhibiting decrease in width and increase in height of the distribution.

Conclusions

An attempt was made to create a optical feedback loop, experimentally, that would reproduce the output plane of an optical black box to its input as accurately as possible. For this purpose an interferometer was set up. A phase extraction code was written that is capable of taking a inteferogram as input and provide with the phase diagram unwrapped from $[0, 2\pi)$ quite accurately. The code is independent of any parameter and does not involve any post processing. Two sets of runs were performed with a convergent lens in the black box. The first run suffered from problems of involving one visible range mirror in the path which led to loss of significant intensity. Also, imaging the first order led to cumulative errors in phase to make the outcomes inconclusive. The second run, was performed with corrected set up and added grating. Only ole loop was ran, mainly due too the geometric parameters of the set-up, which restricted the possible value of the grating added in a far from perfect range, to have achieved a conclusive result. However, the data is qualitatively indicative of modelling a convergent beam.